

# Recounting the FANTOM Cage Associated Transcriptome

**Eddie-Ludy Imada<sup>1,2,+</sup>, Diego Fernando Sanchez<sup>1,+</sup>, Leonardo Collado-Torres<sup>3</sup>, Christopher Wilks<sup>4</sup>, Tejasvi Matam<sup>1</sup>, Wikum Dinalankara<sup>1</sup>, Aleksey Stupnikov<sup>1</sup>, Francisco Lobo-Pereira<sup>5</sup>, Chi-Wai Yip<sup>6</sup>, Kayoko Yasuzawa<sup>6</sup>, Naoto Kondo<sup>6</sup>, Masayoshi Itoh<sup>7</sup>, Harukazu Suzuki<sup>6</sup>, Takeya Kasukawa<sup>6</sup>, Chung-Chau Hon<sup>6</sup>, Michiel JL de Hoon<sup>6</sup>, Jay W Shin<sup>6</sup>, Piero Carninci<sup>6</sup>, FANTOM consortium , Andrew E Jaffe<sup>3,8,9</sup>, Jeffrey T Leek<sup>9</sup>, Alexander Favorov<sup>1,10</sup>, Gloria R Franco<sup>2</sup>, Ben Langmead<sup>4,9,\*</sup>, and Luigi Marchionni<sup>1,\*,+,a</sup>**

<sup>1</sup>Department of Oncology, Johns Hopkins University School of Medicine, Baltimore, MD, USA

<sup>2</sup>Departamento de Bioquímica e Imunologia, ICB, Universidade Federal de Minas Gerais, Belo Horizonte, MG, Brazil

<sup>3</sup>Lieber Institute for Brain Development, Baltimore, MD, USA

<sup>4</sup>Department of Computer Science, Johns Hopkins University, Baltimore, MD, USA

<sup>5</sup>Departamento de Biología General, ICB, Universidade Federal de Minas Gerais, Belo Horizonte, MG, Brazil

<sup>6</sup>RIKEN Center for Integrative Medical Sciences, Yokohama, Japan

<sup>7</sup>RIKEN, Preventive Medicine and Diagnostic Innovation Program, Yokohama, Japan

<sup>8</sup>Department of Mental Health, Johns Hopkins Bloomberg School of Public Health, Baltimore, MD, USA

<sup>9</sup>Department of Biostatistics, Johns Hopkins Bloomberg School of Public Health, Baltimore, MD, USA

<sup>10</sup>Laboratory of Systems Biology and Computational Genetics, VIGG RAS, Moscow, RF

<sup>\*,+</sup>These authors contributed equally to this work

<sup>a</sup>Correspondence to Luigi Marchionni: [marchion@jhu.edu](mailto:marchion@jhu.edu)

## ABSTRACT

Long non-coding RNAs (lncRNAs) have emerged as key coordinators of biological and cellular processes. Characterizing lncRNA expression across cells and tissues is key to understanding their role in determining phenotypes including human diseases. We present here FC-R2, a comprehensive expression atlas across a broadly-defined human transcriptome, inclusive of over 109,000 coding and non-coding genes, as described in the FANTOM CAGE-Associated Transcriptome (FANTOM-CAT) study. This atlas greatly extends the gene annotation used in the original *recount2* resource. We demonstrate the utility of the FC-R2 atlas by reproducing key findings from published large studies and by generating new results across normal and diseased human samples. In particular, we (a) identify tissue specific transcription profiles for distinct classes of coding and non-coding genes, (b) perform differential expression analyses across thirteen cancer types, providing new insights linking promoter and enhancer lncRNAs expression to tumor pathogenesis, and (c) confirm the prognostic value of several enhancers in cancer. Comprised of over 70,000 samples, the FC-R2 atlas will empower other researchers to investigate functions and biological roles of both known coding genes and novel lncRNAs. Most importantly, access to the FC-R2 atlas is available from <https://jhbiostatistics.shinyapps.io/recount/>, the *recount* Bioconductor package, and <http://marchionnilab.org/fcr2.html>.

## Introduction

Long non-coding RNAs (lncRNAs) are commonly defined as transcripts devoid of open reading frames (ORFs) longer than 200 nucleotides, which are often polyadenylated. This definition is not based on their function, since lncRNAs are involved in distinct molecular processes and biological contexts not yet fully characterized<sup>1</sup>. Over the past few years, the importance of lncRNAs has clearly emerged, leading to an increasing focus on decoding the consequences of their modulation, studying their involvement in the regulation of key biological mechanisms during development, normal tissue and cellular homeostasis, and in disease<sup>1-3</sup>.

Given the emerging and previously underestimated importance of non-coding RNAs, the FANTOM consortium has initiated the systematic characterization of their biological function. Through the use of Cap Analysis of Gene Expression sequencing (CAGE-seq), combined with RNA-seq data from the public domain, the FANTOM consortium released a comprehensive atlas of the human transcriptome, encompassing more accurate transcriptional start sites (TSS) for coding and non-coding genes, including numerous novel long non-coding genes: the FANTOM CAGE Associated Transcriptome (*FANTOM-CAT*)<sup>4</sup>. We hypothesized that these lncRNAs can be measured in many RNA-seq datasets from the public domain and that they have been so far missed by the lack of a comprehensive gene annotation.

Although the systematic analysis of lncRNAs function is being addressed by the FANTOM consortium in loss of function studies, increasing the detection rate of these transcripts combining different studies is difficult because the heterogeneity of analytic methods employed. Current resources that apply uniform analytic methods to create expression summaries from public data do exist but can miss several lncRNAs because their dependency on a pre-existing gene annotation for creating the genes expression summaries<sup>5,6</sup>. We recently created *recount2*<sup>7</sup>, a collection of uniformly-processed human RNA-seq data, wherein we summarized 4.4 trillion reads from over 70,000 human samples from the Sequence Reads Archive (SRA), The Cancer Genome Atlas (TCGA)<sup>8</sup>, and the Genotype-Tissue Expression (GTEx)<sup>9</sup> projects<sup>7</sup>. Importantly, *recount2* provides annotation-agnostic coverage files that allow re-quantification using a new annotation without having to re-process the RNA-seq data.

Given the unique opportunity to access lastest results to the most comprehensive human transcriptome (the *FANTOM-CAT* project) and the *recount2* gene agnostic summaries, we addressed the previous described challenges building a comprehensive atlas of coding and non-coding gene expression across the human genome: the *FANTOM-CAT/recount2* expression atlas (FC-R2 hereafter). Our resource contains expression profiles for 109,873 putative genes across over 70,000 samples, enabling an unparalleled resource for the analysis of the human coding and non-coding transcriptome.

## Results

### Building the *FANTOM-CAT/recount2* resource

The *recount2* resource includes a coverage track, in the form of a BigWig file, for each processed sample. We built the FC-R2 expression atlas by extracting expression levels from *recount2* coverage tracks in regions that overlapped unambiguous

exon coordinates for the permissive set of *FANTOM-CAT* transcripts, according to the pipeline shown in Figure 1. Since *recount2*'s coverage tracks does not distinguish from between genomic strands, we removed ambiguous segments that presented overlapping exon annotations from both strands (see Methods section and Supp. Methods). After such disambiguation procedure, the remaining 1,066,515 exonic segments mapped back to 109,869 genes in *FANTOM-CAT* (out of the 124,047 starting ones included in the permissive set<sup>4</sup>). Overall, the FC-R2 expression atlas encompasses 2,041 studies with 71,045 RNA-seq samples, providing expression information for 22,116 coding genes and 87,763 non-coding genes, such as enhancers, promoters, and others lncRNAs.

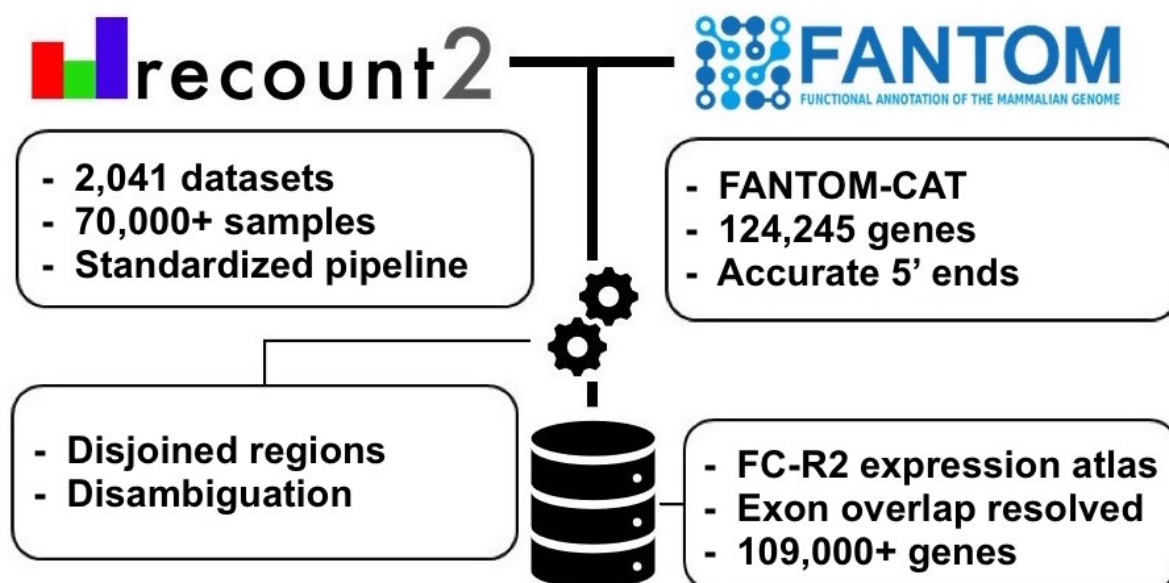


**Figure 1. Overview of the *FANTOM-CAT/recount2* resource development.** FC-R2 leverages two public resources, the *FANTOM-CAT* gene models and *recount2*. FC-R2 provides expression information for 109,873 genes, both coding (22,110) and non-coding (87,693). This latter group encompasses enhancers, promoters, and others lncRNAs.

### Validating the *FANTOM-CAT/recount2* resource

We first assessed how gene expression estimates in FC-R2 compared to previous gene expression estimates from other projects. Specifically, we considered data from the GTEx consortium (v6), spanning 9,662 samples from 551 individuals and 54 tissue types<sup>9</sup>. First, we computed the correlation for the GTEx data between gene expression based on the FC-R2 atlas and on GENCODE (v25) gene model in *recount2*, which has been already shown to be consistent with gene expression estimates from the GTEx project<sup>7</sup>, observing a median correlation  $\geq 0.986$  for the 32,922 genes in common. This result supports the notion that our pre-processing steps to disambiguate overlapping exon regions between strands did not significantly alter gene expression quantification.

Next, we assessed whether gene expression specificity, as measured in FC-R2, was maintained across tissue types. To this end, we selected and compared gene expression for known tissue-specific expression patterns, such as Keratin 1 (*KRT1*), Estrogen Receptor 1 (*ESR1*), and Neuronal Differentiation 1 (*NEUROD1*) (Figure 2). Overall, all analyzed tissue specific

markers presented nearly identical expression profiles across GTEx tissue types between the alternative gene models considered (see Figure 2 and S1), confirming the consistency between gene expression quantification in FC-R2 and those based on GENCODE.

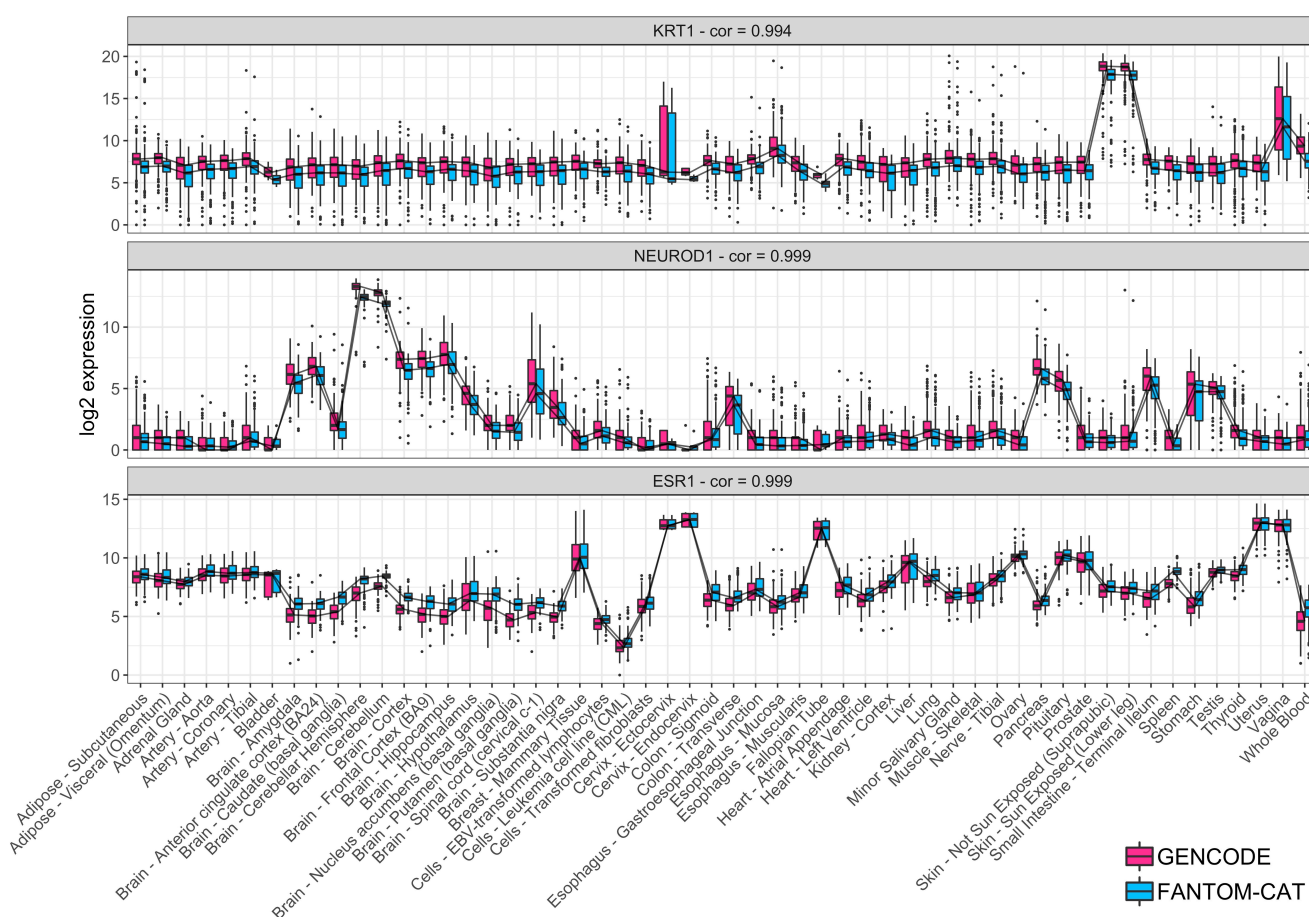


**Figure 2. Tissue specific expression in GTEx.** Log<sub>2</sub> expression for three tissue specific genes (*KRT1*, *NEUROD1*, and *ESR1*) in GTEx data stratify by tissue type using FC-R2 and GENCODE based quantification. Expression profiles are highly correlated and expressed consistently in the expected tissue types (e.g., *KRT1* is most expressed in skin, *NEUROD1* in brain, and *ESR1* in estrogen sensitive tissue types like uterus, Fallopian tubes, and breast). Correlations are shown on top for each tissue marker. Center lines, upper/lower quartiles and Whiskers represents the median, 25/75 quartiles and 1.5 interquartile range, respectively.

### Tissue-specific expression of lncRNAs

It has been shown that, although expressed at a lower level, enhancers and promoters are not ubiquitously expressed and are more specific for different cell types than coding genes<sup>4</sup>. In order to verify this finding, we used GTEx data to assess expression levels and specificity profiles across samples from each of the 54 analyzed tissue types, stratified into four distinct gene categories: coding mRNA, intergenic promoter lncRNA (ip-lncRNA), divergent promoter lncRNA (dp-lncRNA), and enhancers lncRNA (e-lncRNA). Overall, we were able to confirm that these RNA classes are expressed at different levels, and that they display distinct specificity patterns across tissues, as shown for primary cell types by Hon et al.<sup>4</sup>, albeit with more variability

likely due to the increased cellular complexity present in tissues. Specifically, coding mRNAs were expressed at higher levels than lncRNAs (log<sub>2</sub> median expression of 6.6 for coding mRNAs, and of 4.1, 3.8 and 3.1, for ip-lncRNA, dp-lncRNA, and e-lncRNA, respectively). In contrast, the expression of enhancers and intergenic promoters was more tissue-specific (median = 0.41 and 0.30) than what observed for divergent promoters and coding mRNAs (median = 0.13 and 0.09) (Figure 3A). Finally, when analyzing the percentage of genes expressed across tissues by category, we observed that coding genes are, in general, ubiquitous, while lncRNAs are more specific, with enhancers showing the lowest percentages of expressed genes (mean ranging from 88.42% to 41.98%, see Figure 3B), in agreement with the notion that enhancer transcription is tissue specific<sup>10</sup>.

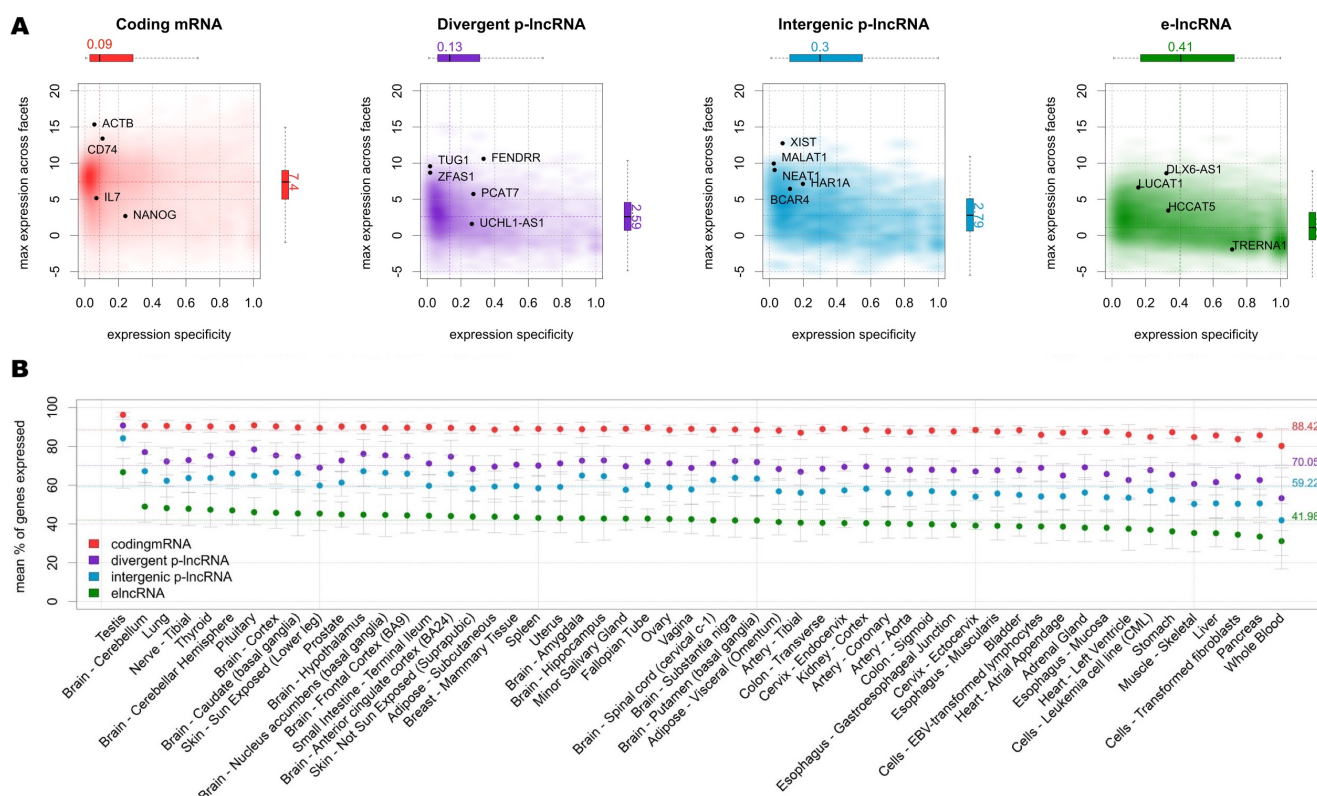


**Figure 3. Expression profiles across GTEx tissues.** **A)** Expression level and tissue specificity across four distinct RNA categories. The Y-axis shows log<sub>2</sub> expression levels representing each gene using its maximum expression in GTEx tissues expressed as transcripts per million (TMP). The X-axis shows expression specificity based on entropy computed from median expression of each gene across the GTEx tissue types. Individual genes are highlighted in the figure panels. **B)** Percentage of genes expressed for each RNA category stratified by GTEx tissue facets. The dots represent the mean among samples within a facet and the error bars represent 99.99% confidence intervals. Dashed lines represent the means among all samples.

### Differential expression analysis of coding and non-coding genes in cancer

We analyzed coding and non-coding genes expression in cancer using TCGA data. To this end, we compared cancer to normal samples separately for 13 tumor types, using FC-R2 re-quantified data. We further identified the differentially expressed genes (DEG) in common across the distinct cancer types (see Figure 4). Overall, the number of DEG varied across cancer types and by gene class, with a higher number of significant coding than non-coding genes (FDR < 0.01, see table 1). Importantly,

a substantial fraction of these genes was exclusively annotated in the *FANTOM-CAT*, suggesting that relying on other gene models would result in missing many potential important genes (see Table 1). We then analyzed the consensus among cancer types. A total of 41 coding mRNAs were differentially expressed across all the 13 tumor types after global correction for multiple testing (FDR < 10<sup>-6</sup>, see Supplementary table S1). For lncRNAs, a total of 28 divergent promoters, four intergenic promoters, and three enhancers were consistently up- or down-regulated across all the 13 tumor types after global correction for multiple testing (FDR < 0.1, see Supplementary tables S2, S3, S4, respectively).

Cancer type	Total	dp-lncRNA		e-lncRNA		ip-lncRNA		mRNA	
		Up	Down	Up	Down	Up	Down	Up	Down
Bile	7010	200 (60)	313 (90)	186 (89)	203 (99)	47 (12)	84 (17)	2658 (106)	3319 (97)
Bladder	7680	344 (125)	319 (87)	140 (68)	149 (67)	65 (19)	82 (7)	3112 (201)	3469 (61)
Breast	15290	753 (291)	721 (202)	656 (377)	583 (305)	207 (50)	178 (32)	6109 (296)	6083 (244)
Colorectal	13685	490 (164)	592 (168)	381 (203)	400 (196)	130 (32)	160 (28)	5538 (371)	5994 (132)
Esophagus	4883	87 (21)	193 (50)	90 (38)	184 (103)	40 (11)	48 (2)	1921 (83)	2320 (77)
Head and Neck	10517	442 (138)	401 (96)	267 (139)	251 (112)	100 (23)	109 (18)	4329 (256)	4618 (53)
Kidney	15697	734 (238)	820 (281)	535 (299)	486 (209)	203 (45)	200 (48)	6349 (525)	6370 (114)
Liver	10554	346 (94)	395 (106)	230 (102)	248 (123)	90 (16)	112 (19)	4164 (174)	4969 (95)
Lung	17143	864 (338)	835 (304)	893 (512)	729 (396)	242 (76)	213 (39)	7523 (532)	5844 (212)
Prostate	13183	686 (287)	654 (218)	418 (254)	452 (214)	175 (55)	167 (30)	5153 (489)	5478 (128)
Stomach	11309	528 (213)	518 (164)	462 (291)	436 (240)	144 (51)	129 (22)	4509 (558)	4583 (89)
Thyroid	14264	752 (284)	804 (318)	527 (295)	594 (332)	161 (39)	174 (47)	5403 (189)	5849 (308)
Uterus	12906	641 (285)	713 (235)	454 (263)	612 (341)	210 (79)	225 (54)	5135 (335)	4916 (181)
Mean	11855	528 (195)	560 (178)	403 (225)	410 (211)	140 (39)	145 (28)	4762 (317)	4909 (138)
St. Dev	3650	237 (102)	218 (89)	225 (137)	189 (107)	67 (23)	55 (16)	1557 (167)	1234 (77)

**Table 1. Differentially expressed genes in cancer.** The table below summarizes the number of significant DEG (FDR  $\leq 0.01$ ) between tumor and normal samples across the 13 cancer types analyzed for each gene class considered (coding mRNA, ip-lncRNA, dp-lncRNA, and e-lncRNA). Counts are reported separately for DEG up- and down-regulated in cancer, and values in parenthesis represents the number of genes exclusively annotated in the *FANTOM-CAT* gene model. Mean and standard deviation across cancer types is shown at the bottom.

Next, we reviewed the literature to assess functional correlates for such consensus genes. Most of the up-regulated coding genes (Supplementary Table S1) participate in cell cycle regulation, cell division, DNA replication and repair, chromosome segregation, and mitotic spindle checkpoints. Most of the consensus down-regulated mRNAs (Supplementary Table S1) are associated with metabolism and oxidative stress, transcriptional regulation, cell migration and adhesion, and with modulation of DNA damage repair and apoptosis.

Three down-regulated dp-lncRNA genes, *RP11-276H19*, *RPL34-AS1*, and *RAP2C-AS1*, were reported to be implicated in cancer (Supplementary Table S2). The first one controls epithelial-mesenchymal transition, the second is associated with

tumor size increase, while the third is associated with urothelial cancer after kidney cancer transplantation<sup>11–13</sup>. Among the up-regulated dp-lncRNAs (Supplementary Table S2), *SNHG1* has been implicated in cellular proliferation, migration and invasion of different cancer types, and to be strongly up-regulated in osteosarcoma, non-small lung cancer, and gastric cancer<sup>14, 15</sup>.

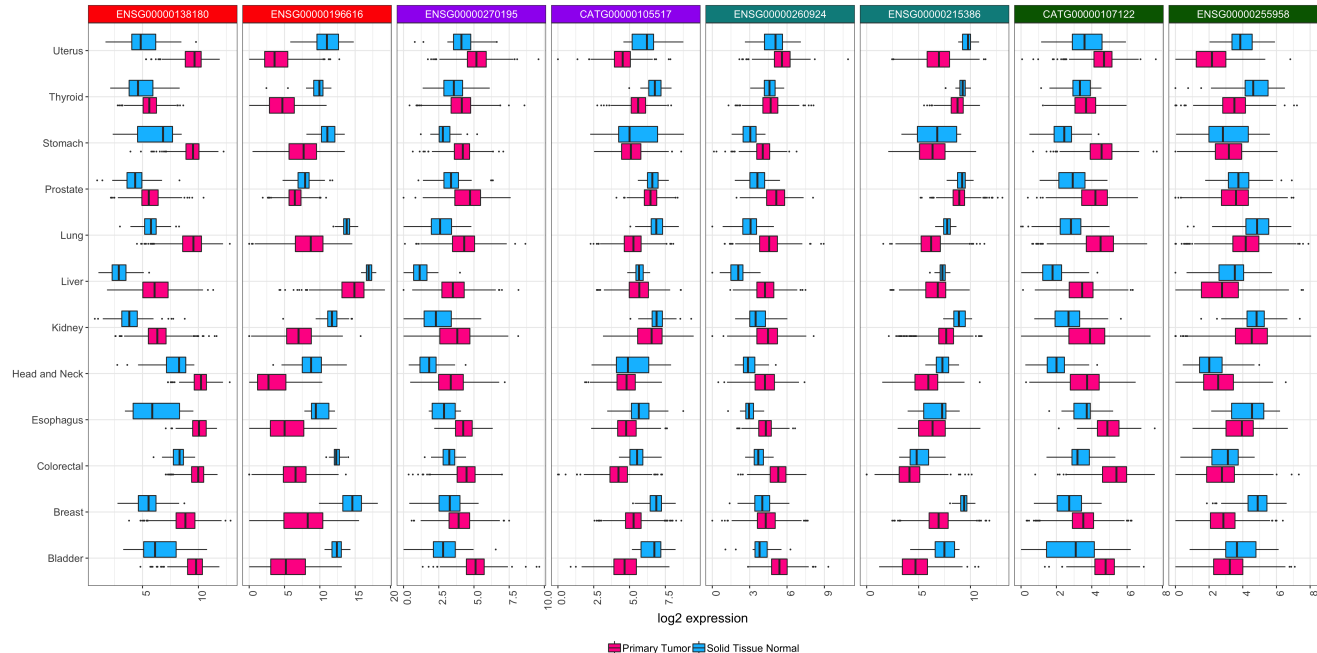


**Figure 4. Differential expression for selected transcripts from distinct RNA classes across tumor types.** Boxplots for selected differential expressed genes between tumor and normal samples across all 13 tumor types analyzed. For each tissue of origin, the most up-regulated (on the left) and down-regulated (on the right) gene for each RNA class is shown. Center lines, upper/lower hinges, and the whiskers respectively represent the median, the upper and lower quartiles, and 1.5 extensions of the interquartile range. Color coding on top of the figure indicates the RNA classes (red for mRNA, purple for dp-lncRNA, cyan for ip-lncRNA, and green for e-lncRNA). These genes were select after global multiple testing correction across all 13 tumor types (see Supplementary Tables S1, S2, S3, and S4)

Among the ip-lncRNAs ubiquitously down-regulated (see Supplementary Table S3), *LINC00478* has been identified in many different tumors types including leukemia, breast, vulvar, prostate, and bladder cancer<sup>16–20</sup>. For instance, in vulvar squamous cell carcinoma, *LINC00478* and *MIR31HG* expressions are correlated and associated with tumor differentiation<sup>17</sup>. Similarly, *LINC00478* down-regulation in ER positive breast cancer is associated with progression, recurrence, and metastasis<sup>18</sup>. In contrast, increased expression of *SNHG17* (an ip-lncRNA, see Supplementary Table S3), was associated with short term survival in breast cancer, and with tumor size, stage, and lymph node metastasis in colorectal cancer<sup>21, 22</sup>. In addition, *AC004463*, another ip-lncRNA (Supplementary Table S3), was found to be up-regulated in liver cancer and metastatic prostate cancer<sup>23</sup>. Despite we did not identify any cancer association for common e-lncRNAs, one among those we identified, *RP5-965F6*, has been previously reported to be up-regulated in late-onset Alzheimer's disease<sup>24</sup>. Furthermore, the enhancers lncRNA class also yielded the lowest number of genes in common among all cancer types, reinforcing the concept that enhancers are expressed in a tissue specific manner (See Figure 3A and Supplementary Table S4).

Finally, we focused more in depth on prostate cancer (PCa) as a prototypical example, and we were able to confirm previous findings for both coding and non-coding genes (see Supplementary Figure S2). For coding genes, we confirmed differential expression for known markers of PCa progression and mortality, like *ERG*, *FOXA1*, *RNASEL*, *ARVCF*, and *SLC43A1*<sup>25,26</sup>. Similarly, we also confirmed differential expression for non-coding genes, like *PCA3*, the first clinically approved lncRNA marker for PCa<sup>27,28</sup>, *PCAT1*, a prostate-specific lncRNA involved in disease progression<sup>29</sup>, *MALAT1*, which is associated with PCa poor prognosis<sup>30</sup>, *CDKN2B-AS1*, an anti-sense lncRNA up-regulated in PCa that inhibits tumor suppressor genes activity<sup>31,32</sup>, and the *MIR135* host gene, which is associated with castration-resistant PCa<sup>33</sup>.

### Enhancer expression levels hold prognostic value

The number of lncRNAs involved in cancer development and progression is rapidly increasing, we therefore analyzed the prognostic value of the lncRNAs we identified in our gene expression differential analysis in TCGA, as well as those previously reported in other studies. To this end, Chen and collaborators have recently surveyed enhancers expression in nearly 9,000 patients from TCGA<sup>34</sup>, using genomic coordinates from the FANTOM5 project<sup>35</sup>, identifying 4,803 enhancers with prognostic potential in one or more TCGA tumor types. We therefore leveraged the FC-R2 atlas to identify prognostic coding and non-coding genes using Univariate Cox proportional hazard models, comparing our results for e-lncRNAs with those reported by Chen and colleagues.

When we considered e-lncRNA expression, we identified a total of 5,382 prognostic e-lncRNAs (FDR  $\leq 0.05$ ), and no single one was associated with survival across all cancer types. Overall, the number of significant prognostic e-lncRNAs varied across tumor types, ranging from 3 in head and neck cancer to 3,850 in kidney cancers (see Supplementary Table S6). Notably, two (out of three) e-lncRNAs from our differential gene expression consensus list across all tumor types were also prognostic. Higher expression of *CATG00000107122* gene was associated with worse prognosis in kidney cancer (Supplementary figure S4b). Overall, despite differences in annotation and quantification (see Supplementary Table S5), we were able to confirm prognostic value for 2,765 e-lncRNAs out of the 4,803 reported by Chen et al<sup>34</sup>, including “enhancer 22” (*ENSG00000272666*), which was highlighted as a promising prognostic marker for kidney cancer (Supplementary Figure S3).

Finally, we analyzed the prognostic value for dp-lncRNAs, ip-lncRNAs, and mRNAs (See Supplementary Tables S7, S8, and S9, respectively), and assessed the survival prognostic potential of our consensus genes across tumor types. Thirty-seven of the 41 coding mRNAs, 22 of the 28 differentially expressed dp-lncRNAs, and two out of the four DE ip-lncRNAs, respectively, were found to be prognostic (See Supplementary Tables S10, S11, S12, and S13). Kaplan-Meier survival curves for one selected DE gene on each RNA subtype evaluated here are shown in supplementary figure S4.

## Discussion

The importance of lncRNAs in cell biology and disease has clearly emerged in the past few years and different classes of lncRNAs have been shown to play crucial roles in cell regulation and homeostasis<sup>36</sup>. For instance, enhancers – a major category of gene regulatory elements, which has been shown to be expressed<sup>35,37</sup> – play a prominent role in oncogenic processes<sup>38,39</sup>.

and other human diseases<sup>40,41</sup>. Despite their importance, however, there is a scarcity of large-scale datasets investigating enhancers and other lncRNA classes, in part due to the technical difficulty in applying high-throughput techniques such as ChIP-seq and Hi-C over large cohorts, and to the use of gene models that do not account for them in transcriptomics analyses. Furthermore, the large majority of the lncRNAs that are already known – and that have been shown to be associated with some phenotype – are still lacking functional annotation.

To address these needs, the FANTOM consortium has first constructed the *FANTOM-CAT* meta-transcriptome, a comprehensive atlas of coding and non-coding genes with robust support from CAGE-seq data<sup>4</sup>, then it has undertaken a large scale project to systematically target lncRNAs and characterize their function using a multi-pronged approach (Ramilowski J, et al., manuscript in review<sup>42</sup>). In a complementary effort, we have leveraged public domain gene expression data from *recount2*<sup>7,43</sup> to create a comprehensive gene expression compendium across human cells and tissues based on the *FANTOM-CAT* gene model, with the ultimate goal of facilitating lncRNAs annotation through association studies. To this end, the FC-R2 atlas is already in use in the FANTOM6 project (<http://fantom.gsc.riken.jp/6/>) to successfully characterize lncRNA expression in human samples (Ramilowski J, et al., manuscript in review<sup>42</sup>).

In order to validate our resource, we have compared the gene expression summaries based on *FANTOM-CAT* gene models with previous, well-established gene expression quantifications, demonstrating virtually identical profiles across tissue types overall and for specific tissue markers. We have then confirmed that distinct classes of coding and non-coding genes differ in terms of overall expression levels and specificity patterns across cell types and tissues. Furthermore, with this approach, we were also able to identify mRNAs, promoters, enhancers, and other lncRNAs that are differentially expressed in cancer, both confirming previously reported findings, and identifying novel cancer genes exclusively annotated in the *FANTOM-CAT* gene model, which have been therefore missed in prior analyses with TCGA data. Finally, we also analyzed the prognostic value of the coding and non-coding genes we identified, and confirmed survival associations in TCGA for measurable enhancers.

Collectively, by confirming findings reported in previous studies, our results demonstrate that the FC-R2 gene expression atlas is a reliable and powerful resource for exploring both the coding and non-coding transcriptome, providing compelling evidence and robust support to the notion that lncRNA gene classes, including enhancers and promoters, despite not being yet fully understood, portend significant biological functions. Our resource, therefore, constitutes a suitable and promising platform for future large scales studies in cancer and other human diseases, which in turn hold the potential to reveal important cues to the understanding of their biological, physiological, and pathological roles, potentially leading to improved diagnostic and therapeutic interventions.

Finally, all results, data, and code from the FC-R2 atlas are available as a public tool. With uniformly processed expression data for over 70,000 samples and 109,873 genes ready to analyze, we want to encourage researchers to dive deeper into the study of ncRNAs, their interaction with coding and non-coding genes, and their influence on normal and disease tissues. We hope this new resource will help paving the way to develop new hypotheses that can be followed to unwind the biological role of the transcriptome as a whole.

## Methods

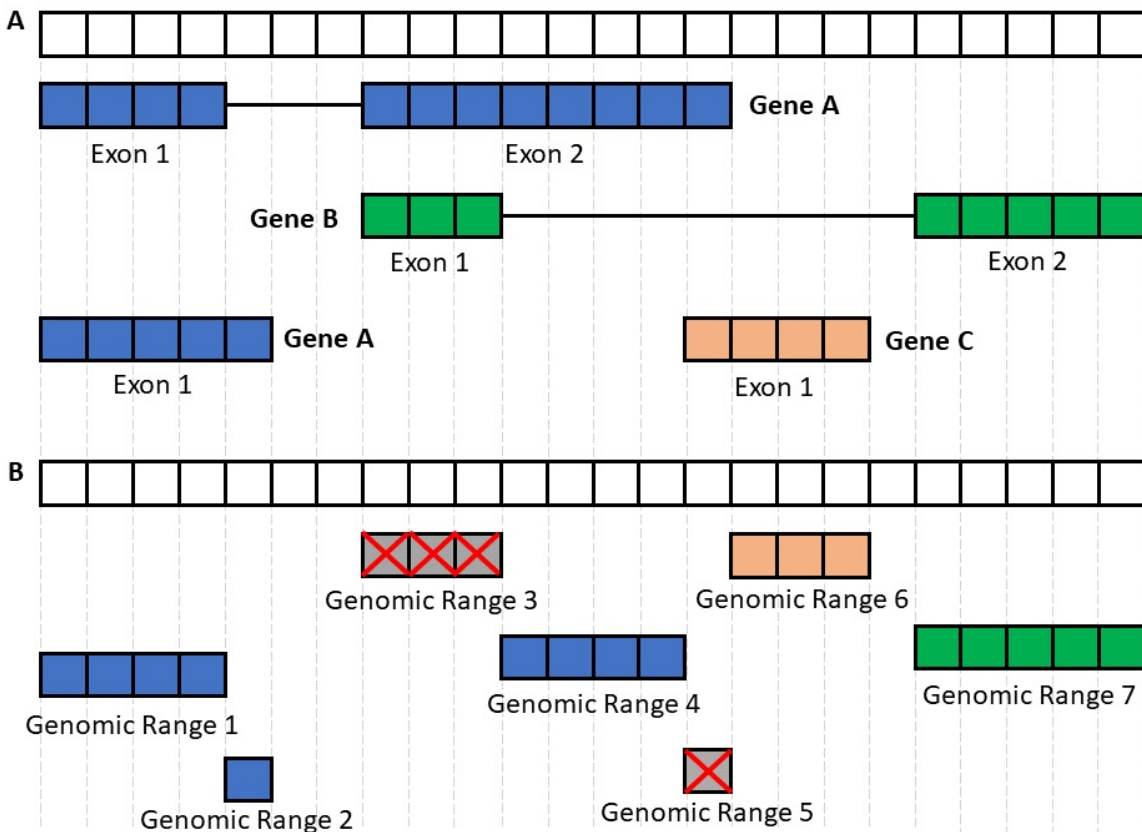


**Figure 5. Processing the FANTOM-CAT genomic ranges.** This figure summarizes the disjoining and exon disambiguation processes performed before extracting expression information from *recount2* using the *FANTOM-CAT* gene models. **A)** Representation of a genomic segment containing 3 distinct, hypothetical genes: gene A having two isoforms, and genes B and C with one isoform each. Each box can be interpreted as one nucleotide along the genome. Colors indicate the 3 different genes. **B)** Representation of disjoint exon ranges from example in Panel A. Each feature is reduced to a set of non-overlapping genomic ranges. The disjoint genomic ranges mapping back to two or more distinct genes are removed (crossed grey boxes). After removal of ambiguous ranges, the expression information for remaining ones is extracted from *recount2* and summarized at the gene level.

### Data and pre-processing.

The FANTOM CAT gene catalog (permissive set) was obtained from the FANTOM consortium within the frame of the FANTOM6 project (Ramilowski J, et al., manuscript in review<sup>42</sup>). This catalog accounts for 124,245 genes supported by CAGE peaks and it includes those described by Hon et al.<sup>4</sup>. In order to remove ambiguity due to overlapping among exons from distinct genes, the BED files containing the coordinates for all genes and exons were processed with the *GenomicRanges* R/Bioconductor package<sup>44</sup> to obtain exon coordinates disjoining. To avoid losing strand information from annotation we processed data using a two-step approach by first disjoining overlapping segments on the same strand and then across strands (Figure 5). The genomic ranges (disjoint exons segments) that mapped back to more than one gene were discarded. The expression values for these ranges

were then quantified using *recount.bwtool*<sup>45</sup> (code at [https://github.com/LieberInstitute/marchionni\\_projects](https://github.com/LieberInstitute/marchionni_projects)). The resulting expression quantification were processed to generate RangedSummarizedExperiment objects compatible with the *recount2* framework<sup>7,43</sup> (code available from <https://github.com/eddieimada/fcr2>). Thus, the FC-R2 atlas provides expression information for coding and non-coding genes (including enhancers, divergent promoters, and intergenic lncRNAs) for 9,662 samples from the Genotype-Tissue Expression (GTEx) project, 11,350 samples from TCGA, and over 50,000 samples from the Sequence Read Archive (SRA).

### Correlation with other studies.

To test if the pre-processing steps used for FC-R2 had a major impact on gene expression quantification, we compared our data to the published GTEx expression values obtained from *recount2* (version 2, <https://jhubiostatistics.shinyapps.io/recount/>). Specifically, we first compared the expression distribution of tissue specific genes across different tissue types and then computed the Pearson correlation for each gene in common across the original *recount2* gene expression estimates based on GENCODE and our version based on the FANTOM-CAT transcriptome.

### Expression specificity of tissue facets.

We analyzed the expression level and specificity of each gene stratified by RNA class (i.e. mRNA, e-lncRNA, dp-lncRNA, ip-lncRNA) using the same approach described by Hon et al.<sup>4</sup> (see Supplementary Methods). Briefly, overall expression levels for each gene were represented by the maximum transcript per million (TPM) values observed across all samples within each tissue type in GTEx. Gene specificity was based on the empirical entropy computed using the mean expression value across tissue types. The 99.99 percent confidence intervals for the expression of each category by tissue type were calculated based on TPM values. Genes with a TPM greater than 0.01 were considered expressed.

### Identification of differentially expressed genes.

We analyzed differential gene expression in 13 cancer types, comparing primary tumor with normal samples using TCGA data from the FC-R2 atlas. Gene expression summaries for each cancer type were split by RNA class (coding mRNA, intergenic promoter lncRNA, divergent promoter lncRNA, and enhancer lncRNA) and then analyzed independently. A generalized linear model approach coupled with empirical Bayes moderation of standard errors<sup>46</sup> was used to identify differentially expressed genes between groups. The model was adjusted for the three most relevant coefficients for data heterogeneity as estimated by surrogate variable analysis (SVA)<sup>47</sup>. Correction for multiple testing was performed across RNA classes by merging the resulting p-values for each cancer type and applying the Benjamini-Hochberg method<sup>48</sup>.

### Prognostic analysis.

To evaluate the prognostic potential of the genes in FC-R2, we performed univariate Cox proportional regression analysis separately for each RNA classes (22106 mRNAs, 17,404 e-lncRNAs, 6,204 dp-lncRNAs, and 1,948 ip-lncRNAs) across each of the 13 TCGA cancer types with available survival follow-up. Genes with FDR equal or less than 0.05, using Benjamini-

Hochberg correction<sup>48</sup> within the cancer type and RNA class, were deemed as significant prognostic factors. We further analyzed the prognostic value of the consensus genes we identified comparing tumors to normal samples by intersecting the corresponding gene lists with those obtained by Cox proportional regression. Finally, in order to compare the results from prognostic analyses, we obtained data on enhancers position and prognostic potential from Chen et al. original publication<sup>34</sup> and performed a liftover to the hg38 genome assembly to match FC-R2 coordinates.

## Data Availability

All data is available from <http://marchionnilab.org/fcr2.html>. Expression data can be directly accessed through <https://jhubiostatistics.shinyapps.io/recount/> and the *recount* Bioconductor package (v1.9.5 or newer) at <https://bioconductor.org/packages/recount> as *RangedSummarizedExperiment* objects organized by The Sequence Read Archive (SRA) study ID. The data can be loaded using R-programming language and is ready to be analyzed using Bioconductor packages or the data can be exported to other formats for use in another environment.

## Code Availability

All code used in this manuscript is available for reproducibility and transparency at: <https://github.com/eddieimada/fcr2> and [https://github.com/LieberInstitute/marchionni\\_projects](https://github.com/LieberInstitute/marchionni_projects).

## Acknowledgements

This publication was made possible though support from the NIH-NCI grants P30CA006973 (L.M. and A.F.), 1U01CA231776 (W.D. and L.M.), and R01CA200859 (W.D. and L.M.), NIH-NIGMS grant R01GM118568 (C.W. and B.L.), R21MH109956-01 (L.C.T. and A.E.J.), and the Department of Defense (DoD) office of the Congressionally Directed Medical Research Programs (CDMRP) award W81XWH-16-1-0739 (E.L.I. and L.M.), Russian Academic project 0112-2019-0001 (A.F.), Fundação de Amparo à Pesquisa do Estado de Minas Gerais award BDS-00493-16 (E.L.I and G.R.F.). *recount2* and FC-R2 are hosted on SciServer, a collaborative research environment for large-scale data-driven science. It is being developed at, and administered by, the Institute for Data Intensive Engineering and Science (IDIES) at Johns Hopkins University. SciServer is funded by the National Science Foundation Award ACI-1261715. For more information about SciServer, visit <http://www.sciserver.org/>.

## Author contributions statement

L.M. conceived the idea, L.M., E.L.I., A.F. and B.L. designed the study; E.L.I., D.F.S., T.M., W.D., A.S., L.C.T., and L.M. performed the analysis; E.L.I., D.F.S., F.P.L., G.R.F. and L.M. interpreted the results; L.C.T., C.W., C.Y., K.Y., N.K., M.I., H.S., T.K., C.C.H., M.H., J.W.S., P.C. A.E.J., J.T.L. and B.L. provided the data and tools; E.L.I., D.F.S., L.C.T., B.L. and L.M. wrote the manuscript; All authors reviewed and approved the manuscript.

## Disclosure declaration

All authors declare no conflicts of interest.

## References

1. Batista, P. J. & Chang, H. Y. Long noncoding RNAs: cellular address codes in development and disease. *Cell* **152**, 1298–1307 (2013). URL <http://eutils.ncbi.nlm.nih.gov/entrez/eutils/elink.fcgi?dbfrom=pubmed&id=23498938&retmode=ref&cmd=prlinks>. DOI 10.1016/j.cell.2013.02.012.
2. Esteller, M. Non-coding RNAs in human disease. *Nat. reviews Genet.* **12**, 861–874 (2011). URL <https://www.nature.com/articles/nrg3074>. DOI 10.1038/nrg3074.
3. Ling, H. *et al.* Junk DNA and the long non-coding RNA twist in cancer genetics. *Oncogene* **34**, 5003–5011 (2015). URL <http://www.nature.com/articles/onc2014456>. DOI 10.1038/onc.2014.456.
4. Hon, C.-C. *et al.* An atlas of human long non-coding RNAs with accurate 5' ends. *Nat.* **543**, 199–204 (2017). URL <http://www.nature.com/doifinder/10.1038/nature21374>. DOI 10.1038/nature21374.
5. Lachmann, A. *et al.* Massive mining of publicly available RNA-seq data from human and mouse. *Nat Commun* **9**, 1366 (2018).
6. Tatlow, P. J. & Piccolo, S. R. A cloud-based workflow to quantify transcript-expression levels in public cancer compendia. *Sci Rep* **6**, 39259 (2016).
7. Collado-Torres, L. *et al.* Reproducible RNA-seq analysis using recount2. *Nat. Biotechnol.* **35**, 319–321 (2017). URL <http://www.nature.com/doifinder/10.1038/nbt.3838>. DOI 10.1038/nbt.3838.
8. Network, C. G. A. R. *et al.* The Cancer Genome Atlas Pan-Cancer analysis project. *Nat. Genet.* **45**, 1113–1120 (2013). URL <http://eutils.ncbi.nlm.nih.gov/entrez/eutils/elink.fcgi?dbfrom=pubmed&id=24071849&retmode=ref&cmd=prlinks>. DOI 10.1038/ng.2764.
9. GTEx Consortium. The Genotype-Tissue Expression (GTEx) project. *Nat. Genet.* **45**, 580–585 (2013). URL <http://www.nature.com/articles/ng.2653>. DOI 10.1038/ng.2653.
10. Ong, C.-T. & Corces, V. G. Enhancer function: new insights into the regulation of tissue-specific gene expression. *Nat. Rev. Genet.* **12**, 283 (2011).
11. Zhou, M. *et al.* Lncrna-hh strengthen cancer stem cells generation in twist-positive breast cancer via activation of hedgehog signaling pathway. *Stem cells* **34**, 55–66 (2016).
12. Zhao, J. *et al.* Long non-coding rna linc00152 is involved in cell cycle arrest, apoptosis, epithelial to mesenchymal transition, cell migration and invasion in gastric cancer. *Cell cycle* **14**, 3112–3123 (2015).
13. Shang, D., Zheng, T., Zhang, J., Tian, Y. & Liu, Y. Profiling of mrna and long non-coding rna of urothelial cancer in recipients after renal transplantation. *Tumor Biol.* **37**, 12673–12684 (2016).
14. Cao, W.-J., Wu, H.-L., He, B.-S., Zhang, Y.-S. & Zhang, Z.-Y. Analysis of long non-coding rna expression profiles in gastric cancer. *World journal gastroenterology: WJG* **19**, 3658 (2013).

15. Sun, Y. *et al.* The long noncoding rna snhg1 promotes tumor growth through regulating transcription of both local and distal genes. *Oncogene* **36**, 6774 EP – (2017). URL <https://doi.org/10.1038/onc.2017.286>.
16. Emmrich, S. *et al.* Lincrnas monc and mir100hg act as oncogenes in acute megakaryoblastic leukemia. *Mol. cancer* **13**, 1 (2014).
17. Ni, S., Zhao, X. & Ouyang, L. Long non-coding rna expression profile in vulvar squamous cell carcinoma and its clinical significance. *Oncol. reports* **36**, 2571–2578 (2016).
18. Gökmen-Polar, Y. *et al.* Abstract p2-06-05: Linc00478: A novel tumor suppressor in breast cancer (2016).
19. Sun, D. *et al.* Regulation of several androgen-induced genes through the repression of the mir-99a/let-7c/mir-125b-2 mirna cluster in prostate cancer cells. *Oncogene* **33**, 1448 (2014).
20. Li, S. *et al.* Exploring functions of long noncoding rnas across multiple cancers through co-expression network. *Sci. reports* **7**, 754 (2017).
21. Zhao, W., Luo, J. & Jiao, S. Comprehensive characterization of cancer subtype associated long non-coding rnas and their clinical implications. *Sci. reports* **4**, 6591 (2014).
22. Ma, Z. *et al.* Long non-coding rna snhg17 is an unfavourable prognostic factor and promotes cell proliferation by epigenetically silencing p57 in colorectal cancer. *Mol. BioSystems* **13**, 2350–2361 (2017).
23. Zhu, S. *et al.* Genome-scale deletion screening of human long non-coding rnas using a paired-guide rna crispr–cas9 library. *Nat. biotechnology* **34**, 1279 (2016).
24. Humphries, C. E. *et al.* Integrated whole transcriptome and dna methylation analysis identifies gene networks specific to late-onset alzheimer's disease. *J. Alzheimer's Dis.* **44**, 977–987 (2015).
25. Lin, D. W. *et al.* Genetic variants in the LEPR, CRY1, RNASEL, IL4, and ARVCF genes are prognostic markers of prostate cancer-specific mortality. *Cancer Epidemiol Biomarkers Prev* **20**, 1928–1936 (2011). URL <http://cebp.aacrjournals.org/content/20/9/1928.abstract>. DOI 10.1158/1055-9965.EPI-11-0236.
26. Yu, J. *et al.* An integrated network of androgen receptor, polycomb, and TMPRSS2-ERG gene fusions in prostate cancer progression. *Cancer cell* **17**, 443–454 (2010). URL [http://www.sciencedirect.com/science?\\_ob=ArticleURL&\\_udi=B6WWK-503HV0F-7&\\_user=75682&\\_coverDate=05%2F18%2F2010&\\_rdoc=1&\\_fmt=high&\\_orig=gateway&\\_origin=gateway&\\_sort=d&\\_docanchor=&view=c&\\_acct=C000006078&\\_version=1&\\_urlVersion=0&\\_userid=75682&md5=1893cfe1116f128f58fa146786f4e208&searchtype=a](http://www.sciencedirect.com/science?_ob=ArticleURL&_udi=B6WWK-503HV0F-7&_user=75682&_coverDate=05%2F18%2F2010&_rdoc=1&_fmt=high&_orig=gateway&_origin=gateway&_sort=d&_docanchor=&view=c&_acct=C000006078&_version=1&_urlVersion=0&_userid=75682&md5=1893cfe1116f128f58fa146786f4e208&searchtype=a). DOI 10.1016/j.ccr.2010.03.018.
27. Bussemakers, M. J. *et al.* DD3: a new prostate-specific gene, highly overexpressed in prostate cancer. *Cancer Res.* **59**, 5975–5979 (1999).

28. de Kok, J. B. *et al.* DD3(PCA3), a very sensitive and specific marker to detect prostate tumors. *Cancer Res* **62**, 2695–2698 (2002). URL <http://eutils.ncbi.nlm.nih.gov/entrez/eutils/elink.fcgi?dbfrom=pubmed&id=11980670&retmode=ref&cmd=prlinks>.
29. Prensner, J. R. *et al.* Transcriptome sequencing across a prostate cancer cohort identifies PCAT-1, an unannotated lincRNA implicated in disease progression. *Nat. Biotechnol.* **29**, 742–749 (2011). URL <http://www.nature.com/articles/nbt.1914>. DOI 10.1038/nbt.1914.
30. Ren, S. *et al.* Long noncoding RNA MALAT-1 is a new potential therapeutic target for castration resistant prostate cancer. *The J. Urol.* **190**, 2278–2287 (2013). URL <http://eutils.ncbi.nlm.nih.gov/entrez/eutils/elink.fcgi?dbfrom=pubmed&id=23845456&retmode=ref&cmd=prlinks>. DOI 10.1016/j.juro.2013.07.001.
31. Gutschner, T. & Diederichs, S. The hallmarks of cancer: a long non-coding RNA point of view. *RNA Biol* **9**, 703–719 (2012). URL <http://eutils.ncbi.nlm.nih.gov/entrez/eutils/elink.fcgi?dbfrom=pubmed&id=22664915&retmode=ref&cmd=prlinks>. DOI 10.4161/rna.20481.
32. Kotake, Y. *et al.* Long non-coding RNA ANRIL is required for the PRC2 recruitment to and silencing of p15(INK4B) tumor suppressor gene. *Oncogene* **30**, 1956–1962 (2011). URL <https://www.nature.com/articles/onc2010568>. DOI 10.1038/onc.2010.568.
33. Huang, X. *et al.* Exosomal miR-1290 and miR-375 as prognostic markers in castration-resistant prostate cancer. *Eur. urology* **67**, 33–41 (2015). URL <http://linkinghub.elsevier.com/retrieve/pii/S0302283814006873>. DOI 10.1016/j.eururo.2014.07.035.
34. Chen, H., Li, C., Peng, X., Zhou, Z., Weinstein, J. N., Liang, H. A promoter-level mammalian expression atlas. *Cell* **173**, 386–399 (2018).
35. Andersson, R. *et al.* An atlas of active enhancers across human cell types and tissues. *Nat.* **507**, 455–461 (2014). URL <http://eutils.ncbi.nlm.nih.gov/entrez/eutils/elink.fcgi?dbfrom=pubmed&id=24670763&retmode=ref&cmd=prlinks>. DOI 10.1038/nature12787.
36. Quinn, J. J. & Chang, H. Y. Unique features of long non-coding rna biogenesis and function. *Nat. Rev. Genet.* **17**, 47 (2016).
37. Arner, E. *et al.* Transcribed enhancers lead waves of coordinated transcription in transitioning mammalian cells. *Sci. (New York, NY)* (2015). URL <http://eutils.ncbi.nlm.nih.gov/entrez/eutils/elink.fcgi?dbfrom=pubmed&id=25678556&retmode=ref&cmd=prlinks>. DOI 10.1126/science.1259418.
38. Sur, I. & Taipale, J. The role of enhancers in cancer. *Nat. Rev. Cancer* **16**, 483 (2016).
39. Herz, H.-M., Hu, D. & Shilatifard, A. Enhancer malfunction in cancer. *Mol. cell* **53**, 859–866 (2014).
40. Blencowe, B. J. Exonic splicing enhancers: mechanism of action, diversity and role in human genetic diseases. *Trends biochemical sciences* **25**, 106–110 (2000).

41. Hnisz, D. *et al.* Super-enhancers in the control of cell identity and disease. *Cell* **155**, 934–947 (2013).
42. Ramiłowski, J., Wai-Yip, C. & Agrawal, e. a., Saumya. Functional Annotation of Human Long Non-Coding RNAs via Molecular Phenotyping. *Under review* (2019).
43. Collado-Torres, L., Nellore, A. & Jaffe, A. E. recount workflow: Accessing over 70,000 human RNA-seq samples with Bioconductor. *F1000Research* **6**, 1558 (2017). URL <https://f1000research.com/articles/6-1558/v1>. DOI 10.12688/f1000research.12223.1.
44. Lawrence, M. *et al.* Software for computing and annotating genomic ranges. *PLoS Comput. Biol.* **9**, e1003118 (2013). URL <http://eutils.ncbi.nlm.nih.gov/entrez/eutils/elink.fcgi?dbfrom=pubmed&id=23950696&retmode=ref&cmd=prlinks>. DOI 10.1371/journal.pcbi.1003118.
45. Ellis, S. E., Collado-Torres, L., Jaffe, A. & Leek, J. T. Improving the value of public RNA-seq expression data by phenotype prediction. *Nucleic Acids Res.* **46**, e54–e54 (2018). URL <https://doi.org/10.1093/nar/gky102>. DOI 10.1093/nar/gky102. <http://oup.prod.sis.lan/nar/article-pdf/46/9/e54/24829382/gky102.pdf>.
46. Smyth, G. K. Linear models and empirical bayes methods for assessing differential expression in microarray experiments. *Stat. applications genetics molecular biology* **3**, Article3 (2004). URL <http://www.ncbi.nlm.nih.gov/pubmed/16646809?dopt=abstract>. DOI 10.2202/1544-6115.1027.
47. Leek, J. T. & Storey, J. D. Capturing heterogeneity in gene expression studies by surrogate variable analysis. *PLoS genetics* **3**, 1724–1735 (2007). URL <http://www.plosgenetics.org/article/info%3Adoi%2F10.1371%2Fjournal.pgen.0030161>. DOI 10.1371/journal.pgen.0030161.
48. Benjamini, Y. & Hochberg, Y. Controlling the false discovery rate: a practical and powerful approach to multiple testing. *J. Royal Stat. Soc. Series B*, **57**, 289–300 (1995). URL [http://www.dm.uba.ar/materias/analisis\\_expl\\_y\\_conf\\_de\\_datos\\_de\\_exp\\_de\\_marrays\\_Mae/2006/1/teoricas/FDR%201995.pdf](http://www.dm.uba.ar/materias/analisis_expl_y_conf_de_datos_de_exp_de_marrays_Mae/2006/1/teoricas/FDR%201995.pdf).
49. Buja, A. & Eyuboglu, N. Remarks on parallel analysis. *Multivar. behavioral research* **27**, 509–540 (1992).
50. Kassambara, A. & Kosinski, M. *survminer: Drawing Survival Curves using 'ggplot2'* (2018). URL <https://CRAN.R-project.org/package=survminer>. R package version 0.4.3.